RSC Advances

Volume 1 | Number 1 | Jan 2013 | Pages 1–100

RSC Advances

www.rsc.org/advances

ROYAL SOCIETY OF CHEMISTRY

ROYAL SOCIETY OF CHEMISTRY

www.rsc.org/advances

Mechanical properties of polycrystalline boron-nitride nanosheets

Bohayra Mortazavi [*, 1, 2] and Gianaurelio Cuniberti[1, 2, 3, 4]

[1]*Institute for Materials Science and Max Bergman Center of Biomaterials, TU Dresden, 01062 Dresden, Germany*
[2]*Dresden Center for Computational Materials Science, TU Dresden, 01062 Dresden, Germany*
[3]*Center for Advancing Electronics Dresden, TU Dresden, 01062 Dresden, Germany*
[4]*Center for Transport and Devices of Emergent Materials, TU Dresden, 01062 Dresden, Germany*

Abstract

First molecular dynamics (MD) study was conducted to explore mechanical-failure response of ultra-fine grained single-layer boron-nitride films. We used MD simulations to construct relatively large molecular models of polycrystalline structures with random grain configurations. By applying uniaxial tensile loading, we then studied the grain size effect on the mechanical response of polycrystalline boron-nitride nanosheets. Our results reveal that by decreasing the grain size, the elastic modulus of polycrystalline films decrease gradually. Interestingly, our MD results reveal that ultra-fine grained samples could present a tensile strength of around half of the pristine films. Our investigation suggests that experimentally fabricated polycrystalline boron nitride nanosheets can exhibit remarkably high mechanical properties.

*Corresponding author (Bohayra Mortazavi): bohayra.mortazavi@nano.tu-dresden.de

Tel: +49-176-68195567

Fax: +49-351-46331422

1. Introduction

Recent advances in the fabrication of two-dimensional materials with exceptional properties such as graphene [1, 2] and hexagonal boron-nitride (h-BN) [3, 4] sheets have attracted remarkable attention. Graphene and h-BN both have honeycomb atomic lattice which propose them as the best candidates to be heterogeneously integrated for electronics applications. Graphene presents exceptionally high thermal conductivity [5] and mechanical [6] properties that outperforms all other known materials. The attractive point of h-BN in comparison with graphene for electronic applications is due to its electrically insulating properties with a wide band gap of ~5.5 eV [7], whereas the graphene does no present a band gap and is categorized as a semi-metal material. Boron-nitride nanostructures also present high thermal conductivity [8], deep ultraviolet photon emission [9], considerable mechanical properties [10] and piezoelectricity [11]. Accordingly, the fabrication of heterogeneous structures on the basis of electrically insulating h-BN and semi-metal graphene is currently considered as a promising approach to reach to a semiconducting material [12] with high mechanical and thermal properties. On the other side, combination of high thermal and mechanical properties along with planar geometry also proposes the h-BN as a promising candidate for the reinforcement of polymeric materials [13, 14]. Since the h-BN is insulator, reinforcement of electrically non-conductive polymers with h-BN could be considered as an effective way to fabricate an electrically insulating and a highly thermal conductive polymer nanocomposite material, best suited as a building block in nanoelectronics in response to heat dissipation concerns.

Like all other known materials, properties of boron-nitride nanosheets could be also affected by existence of defects. It is worth mentioning that the defects in materials are principally formed during the fabrication process. Currently, the chemical vapor deposition (CVD) technique is the only way for producing large-scale boron-nitride nanosheets [15-18]. Crystal growth during the CVD method leads to the formation of grain boundaries where two grains meet each other, resulting in polycrystalline structures. Grain boundaries consist of different types of topological defects. These defects along the grain boundaries act as dislocation cores that raise the stress concentration, which consequently affect the mechanical response. Moreover, these defects also cause the phonon scattering along the grain boundaries resulting in lower thermal conductivity of the polycrystalline structures in comparison with single-crystalline samples [19]. Accordingly, comprehensive understanding of grain boundary effects on the boron-nitride nanosheets mechanical and thermal properties is of a crucial importance.

Because of exceptional properties of graphene, the majority of the theoretical and experimental studies have been focused on the polycrystalline graphene structures [20-23] and there exist only few studies concerning the polycrystalline h-BN structures. Recent first principles calculations by Liu et al. [24] indicate several possible structures for h-BN grain boundaries, and electronic structure calculations predict a change in band gap by 38% due to additional states along the grain boundaries. The theoretical calculations [24] suggest that the grain boundaries in polycrystalline h-BN not only comprise the well known pentagon-heptagon pairs (5/7) but they also include square-octagon pairs (4/8). However, most recent transmission electron microscope study of CVD grown h-BN films reveals that the grain boundaries in h-BN are mainly consisting of pentagon-heptagon pairs [25]. It was observed that these pentagon-heptagon pairs include homonuclear boron−boron or nitrogen−nitrogen bonds, which are higher in energy than the heteronuclear boron−nitrogen bonds in the surrounding lattice [25]. To the best of our knowledge, mechanical properties of polycrystalline h-BN films have been studied neither theoretically nor experimentally. Accordingly, the objective of this study is to perform molecular dynamics (MD) simulations to provide detailed information concerning the mechanical response of polycrystalline single-layer boron-nitride sheets. To this aim, we developed a methodology for the construction of relatively large polycrystalline h-BN structures with random grain configurations. Then, the constructed models were subjected to uniaxial tensile loading condition to acquire the stress-strain response. Our molecular modeling reveals that CVD grown h-BN films can exhibit noticeably high mechanical properties.

2. Molecular dynamics modeling

All molecular dynamics simulations in this study were performed using LAMMPS (Large-scale Atomic/Molecular Massively Parallel Simulator) [26] package. For the modeling of interactions between boron–boron and nitrogen–nitrogen atoms, we used Tersoff potential [27] parameters proposed by Matsunaga et al. [28]. Accordingly, the Tersoff potential parameters for boron–nitrogen interactions were calculated using Eq. (1e) in Ref. [27].

During the fabrication of h-BN films using the CVD method, the growth along arbitrary crystal orientations is initiated at several nucleation sites simultaneously. These nucleation sites could be considered as initial grains that their growths result in the construction of a polycrystalline structure. In order to simulate such a growth mechanism, we developed a program that creates a preselected number of randomly and uniformly distributed nucleation sites on a plane with predefined dimensions. By assuming a square geometry for an equivalent average grain in a polycrystalline sheet, the grain size in this study is defined by the $\sqrt{\frac{L^2}{N}}$, where L is the plane length and N is the number of grains in the plane. Therefore, for a plane with 50 nm length and 25 grains, the equivalent grain size would be 10 nm. Then, for each nucleation site a random angle between -60° to 60° was assigned which defines the crystal growth orientation with respect to the armchair direction. In the next step, the growth of nucleation sites were performed using an iterative process in which any of the missing neighbors of a boundary atom can appear with the same probability. The further growth of a grain from a boundary atom is terminated when it meets with another atom from the neighboring grain with distance below 0.1 nm or if it was already bonded with three atoms. The growth of polycrystalline structure is finished when all grains meet with their neighbors and there is no possibility for any additional atom to be included in a lattice. The constructed models in this study are periodic which means that if one puts these samples side by side together no mismatch would be observed. It is worth mentioning that in order to have perfect uniaxial loading condition, the structures must be periodic to accurately apply the periodic boundary conditions. This is due to the fact that in the evaluation of mechanical properties, any kind of fixing of atomic positions as boundary conditions could result in local stress concentration which would consequently affect the accuracy of simulation results.

After creating initial positions for boron and nitrogen atoms, MD simulations were used to form the grain boundaries. We note that limited reactivity of Tersoff potentials does not allow the formation of complex grain boundaries. Therefore, in this study we used a similar methodology as that explained in the work by Kotakoski and Meyer [29] for the construction of polycrystalline graphene structures. To this aim, we replaced boron and nitrogen atoms with carbon atoms and then we used the second-generation reactive empirical bond order (REBO) potential [30] for the modeling of inter-atomic interactions. The initial structure was first equilibrated at 300 K for 10 ps using Nosé-Hoover thermostat method (NVT). Then, the structure was uniformly heated to 3000 K using the NVT method for 40 ps. In the next step, the temperature of the system was kept at 3000 K using the NVT method for another 40 ps. The high mobility of atoms at 3000 K let them to rearrange their position to form the grain boundaries and grain boundary junctions. At this stage, the grain boundaries are formed and by cooling the system to room temperature the desired structure is prepared. After creation of polycrystalline structures, we replaced the carbon atoms with native boron and nitrogen atoms to obtain polycrystalline h-BN.

In the molecular dynamics modeling of uniaxial tensile of polycrystalline h-BN films at room temperature, periodic boundary conditions were applied in planar directions to remove finite length effect. For the loading conditions, the periodic simulation box size along the loading direction was increased by a constant engineering strain rate at every simulation time step. In this study, the time increment of the simulations was set at 0.2 fs and the engineering strain rate of 10^9 s^{-1} was applied for the modeling of deformation process. Engineering strain at each time step was calculated by multiplying the total time of loading step by the applied engineering strain rate. Since we deal with single-layer films, the stress in the sheet thickness is zero. Therefore, the periodic simulation box along the sample width was altered during the loading step using the Nosé-Hoover barostat and thermostat method (NPT) in order to guarantee the uniaxial stress condition. Virial stresses at each strain level were calculated to obtain engineering stress-strain response. In the calculation of stress, we assumed the thickness of 0.33 nm which is on the basis of multi-layer hexagonal boron-nitride thickness [31].

3. Results and discussions

In Fig. 1, three samples of constructed polycrystalline h-BN films with equivalent average grain sizes of (a) 10 nm with 25 grains, (b) 5 nm with 25 grains and (c) 2 nm with 144 grains are illustrated. In this study, we developed relatively large polycrystalline films with 24000 to around 100000 atoms consisting of 25 up to 144 grains. As it could be observed, the grain boundaries and grain boundary junctions are accurately formed. For the large grain size of 10 nm and 5 nm, the formed grain boundaries are mainly consisting of pentagon-heptagon and pentagon-octagon pairs and point vacancies. In these cases, the formation of square-octagon pairs is strictly limited. However, for the polycrystalline sample with average grain size of 2 nm, we could observe all combinations of square, pentagon, heptagon and octagon rings along the formed grain boundaries.

Since our aim is to study the mechanical response of polycrystalline h-BN films in which the grains are randomly oriented, we first investigate the mechanical properties of defect-free h-BN films along different loading directions. We note that a honeycomb structure has a symmetry angle of 30º and the chirality angles of 0º and 30º are commonly called as armchair and zigzag directions, respectively. In our modeling, we also study the tensile response of h-BN films along two different chirality angles of 10° and 20° with respect to the armchair direction. The obtained stress-strain curves of defect-free h-BN films subjected to uniaxial loading conditions along four different loading chirality directions from 0º to 30º are illustrated in Fig. 2. The acquired results show that the defect-free h-BN presents higher elastic modulus along the armchair directions than zigzag directions which is in agreement with recent density functional theory (DFT) calculations [33]. Our MD results suggest that the pristine h-BN films present elastic modulus of 800-850 GPa and tensile strength of 150±15 GPa at corresponding failure strain of 0.3±0.03, all depending on the loading direction. The calculated elastic modulus is close to the first principles predictions of 845 GPa [33] and 770-780 GPa [34] for pristine h-BN. It is worth mentioning that the theoretical elastic modulus of armchair boron-nitride nanotubes were reported to be 810 GPa by Kudin et al. [35] and 840-880 GPa by Hernández et al. [36]. Our MD results for failure strain is also in agreement with the quantum calculation results of 0.3 [33] and 0.18-0.29 [34] for defect-free h-BN films. However, the calculated tensile strength by the MD method is higher than first principles estimation of 88-102 GPa [33].

The MD results for stress-strain responses of polycrystalline h-BN films with equivalent average grain sizes of 2 nm and 10 nm are illustrated in Fig. 3. In this study, the calculations for a particular grain size were performed for 4 different samples with different initial grain configurations in order to have better understanding with respect to the statistical variation of our MD results. The results depicted in Fig. 3 show distinct differences for the stress-strain responses of two studied grain sizes. Interestingly, the obtained results for the large grain size of 10 nm are coinciding and only limited variations for the tensile strength and the corresponding failure strain could be observed for different grain configurations. On the other side, for the small grain size of 2 nm we could observe considerably more variations in the predicted tensile strength and failure strain for different grain distributions.

In Fig. 4, MD predictions for elastic modulus, tensile strength and ultimate strain of polycrystalline h-BN films as a function of grain size are illustrated. As an overall trend, we found that by decreasing the grain size in polycrystalline structures, the elastic modulus and tensile strength decrease while the strain at failure increases. The calculated elastic modulus of polycrystalline sample with the average grain size of 10 nm is lower than that of the defect-free h-BN sheet by around 10%. This observation reveals insignificant effect of grain size on the elastic modulus of polycrystalline h-BN films when the grain size is higher than 10 nm. We note that the experimental results show that the mean elastic modulus of polycrystalline graphene sheets decreases only slightly by around 3% in comparison with defect-free graphene [22]. The MD results suggest that the decreasing trend in elastic modulus of polycrystalline h-BN sheets becomes more considerable for the grain sizes smaller than 5 nm. Amazingly, the elastic modulus of the polycrystalline sample with grain size of 2 nm is found to be only by 40% difference with that of the pristine h-BN.

In contrast with the obtained results for elastic modulus, considerable variations in the MD results for tensile strength and corresponding failure strain could be observed. These variations in the tensile strength and the corresponding ultimate strain could be explained by the stochastic nature of failure occurrence in the polycrystalline and defective structures. We note that the grain boundaries in polycrystalline h-BN films act as sources for stress concentrations and cracks nucleation as well, resulting in reduction of tensile strength in comparison with single-crystalline structures. In the case of tensile strength, we found an overall decreasing trend as the grain size decreases. However, the MD results reveal that the ultimate strength of polycrystalline samples with grain size of 5 nm to 10 nm are almost constant and varies around 80 GPa. Interestingly, the MD results for the tensile strength of polycrystalline h-BN films with grain size of 10 nm and 2 nm are respectively, around 55% and 45% of our prediction for pristine structure.

On the other hand, our results depicted in Fig. 4 suggest that the failure strain of polycrystalline h-BN films increases gradually by decreasing the grain size. In this case, we found that the mean ultimate strain of samples with average grain size of 2 nm is around 35% higher than that for the samples with average grain size of 10 nm. This increasing trend in the ultimate strain for smaller grain sizes is in agreement with the MD results for polycrystalline graphene [26]. This finding is interesting since one could expect a decreasing trend for ultimate strain due to the fact that the results for ultimate strain of largest studied grain size in our work is lower than that of the single-crystalline h-BN sheet. We remind that the grain boundaries present weakened mechanical properties in comparison with atoms inside the grains. Therefore, in a polycrystalline h-BN sample, the material response is not uniform and gradients in materials response exist depending on the distance from grain boundaries. However, as the grain size decreases, the ratio of atoms along the grain boundaries to the total numbers of atoms increases. This way, by decreasing the grain size (Fig. 1), defective zones more uniformly extend throughout the sample making the materials response more homogeneous. In this case, the material is softened and because of its homogenous structure it could flow more uniformly during the loading condition resulting in a higher ultimate strain. It is worth mentioning that the ideal homogeneous structure for h-BN belongs to defect-free sample which consequently presents the maximum ultimate strain.

Our MD modeling of uniaxial tension of defect-free h-BN films reveals that the specimen extends uniformly and remains undamaged up to the ultimate strength point. In this case, the tensile strength is a point in which the first debonding occurs between two adjacent boron and nitrogen atoms. This initial debonding forms a crack which rapidly propagates and leads to the sample rupture. In Fig. 5, we plot the deformation process of a polycrystalline h-BN film with an equivalent average grain size of 10 nm at various stages of loading. As it is shown in Fig. 5a, at strain levels relatively far from the failure strain, several voids form along the grain boundaries throughout the sample. These voids are initially formed by debonding of homonuclear boron−boron or nitrogen−nitrogen bonds. However, the growths of these voids along the crack tips are prohibited as they meet with heteronuclear boron−nitrogen bonds. In this case, by rearrangement of atomic positions, the crack tips become more smooth which consequently reduce the stress concentration and help the specimen to endure for longer strain levels. Our MD results for ruptured samples reveal that these initial voids are stabilized in the structure (Fig. 5f). By increasing the strain levels, more voids form along the specimen. The tensile strength is typically a point that a previously formed crack along a grain boundary (Fig. 5b) propagates rapidly by breaking the boron-nitrogen bonds resulting in a characteristic sharp decrease in the stress-strain response. This crack initially propagates only along a grain boundary (Fig. 5c and Fig. 5d) and as it meets with a grain boundary junction it also propagates into the bulk grains (Fig. 5e). This observation clearly suggests the comparable strength of grain boundaries in comparison with defect-free bulk material, otherwise the crack growth would only occur along grain boundaries. Such a failure mechanism is similar to recent experimental observation regarding the polycrystalline graphene films [22]. As shown in Fig. 5f, our MD results show that in the ruptured sample the crack edges present irregular shapes.

4. Conclusion

We performed first molecular dynamics modeling of mechanical response of ultra-fine grained polycrystalline hexagonal boron-nitride (h-BN) films. To this aim, we constructed relatively large models of polycrystalline h-BN samples with equivalent grain sizes ranging from 2 nm to 10 nm. The constructed polycrystalline molecular models were then subjected to uniaxial tensile loading to provide detailed information concerning the grain size effect on the mechanical properties of single-layer boron-nitride sheets. As an overall trend, we found that by decreasing the grain size, the elastic modulus and tensile strength decrease and on the other side the strain at failure increases. Our results for ultra-fine grained h-BN films with an average grain size of 10 nm show around 10% and 45% reduction in the elastic modulus and tensile strength, respectively, in comparison with those of defect-free h-BN sheets. Our results suggest that polycrystalline h-BN films with grain sizes of 5 nm to 10 nm could yield extremely high tensile strengths of around 80 GPa which are by two orders of magnitude higher than that of the high strength steels and titanium alloys. The atomistic modeling results for ultra-fine grained samples suggest that the experimentally fabricated polycrystalline h-BN films can present ultra-high elastic modulus and tensile strength. By plotting the deformation process, we elaborately discuss the failure of mechanism of polycrystalline h-BN films. The MD results suggest that at strain levels relatively far from the failure strain, several voids form along the sample by debonding of boron−boron or nitrogen−nitrogen bonds. However, the tensile strength is found to occur in a point in which a previously formed crack along a grain boundary propagates rapidly by breaking the boron-nitrogen bonds resulting in a characteristic sharp decrease in the stress-strain response. This crack initially propagates only along a grain boundary and as it meets with a grain boundary junction it also propagates into the bulk grains. The MD results also show that in the ruptured sample the crack edges present irregular shapes.

Acknowledgment

The financial support by the Saxon State Ministry for Science and the Arts and Center for Advancing Electronics Dresden are gratefully acknowledged. First author greatly appreciates discussions with Dr. Frank Ortman and Dr. Tahereh Ghane at TU-Dresden.

References

[1] Novoselov, K.S., Geim, A.K., Morozov, S.V., Jiang, D., Zhang, Y., Dubonos, S.V., *et al.* Electric field effect in atomically thin carbon films. Science 306, 666–669 (2004).

[2] Novoselov, K.S., Jiang, D., Schedin, F., Booth, T.J., Khotkevich, V.V., Morozov, S.V., *et al.* Two-dimensional atomic crystals. Proc Nat Acad Sci 102,10451–10453 (2005).

[3] Rubio, A., Corkill, J.L., Cohen, M.L. Theory of graphitic boron nitride nanotubes. Phys. Rev. B 49, 5081–5084 (1994).

[4] Chopra, N.G., Luyken, R.J., Cherrey, K., Crespi, V.H., Cohen, M.L., Louie, S.G., *et al.* Boron nitride nanotubes. Science 269, 966–967 (1995).

[5] Ghosh, S., Bao, W., Nika, D.L., Subrina, S., Pokatilov, E.P., Lau, C.N., *et al.* Dimensional crossover of thermal transport in few-layer graphene. Nat. Mater. 9, 555-558 (2010).

[6] Lee, C., Wei, X., Kysar, J.W., Hone, J.. Measurement of the elastic properties and intrinsic strength of monolayer graphene. Science 321, 385–388(2008).

[7] Blasé, X., Rubio, A, Louie, S.G, Cohen, M.L, Stability and band gap constancy of boron nitride nanotubes. Europhys. Lett. 28, 335–340(1994).

[8] Chen, Y., Zou, J., Campbell, S.J, Caer, G.L. Boron nitride nanotubes: pronounced resistance to oxidation. Appl. Phys. Lett.; 84: 2430–2432 (2004).

[9] Kubota, Y., Watanabe, K., Tsuda, O., Taniguchi, T., Deep ultraviolet light-emitting hexagonal boron nitride synthesized at atmospheric pressure. Science 317, 932–934 (2007).

[10] Golberg, D., Costa, P.M.F.G., Lourie, O., Mitome, M., Bai, X. *et al.* Direct force measurements and kinking under elastic deformation of individual multiwalled boron nitride nanotubes. Nano Lett . 7, 2146–2151(2007).

[11] Sai, N., Mele, E.J., Microscopic theory for nanotube piezoelectricity. Phys. Rev. B 68, 241405 (2003).

[12] Levendorf, M.P., Kim, C.J., Brown, L., Huang, P.Y., Havener, R.W., Muller, D.A., Park, J. Graphene and boron nitride lateral heterostructures for atomically thin circuitry. Nature 448, 627-632 (2012).

[13] Mortazavi, B., Ahzi, S. Molecular Dynamics Study on the Thermal conductivity and mechanical properties of boron doped graphene. Solid State Commun. 152, 1503-1507 (2012).

[14] Mortazavi, B., Bardon, J., Ahzi, S. Interphase effect on the elastic and thermal conductivity response of polymer nanocomposite materials: 3D finite element study. Comput. Mat. Sci.69, 100-106 (2013).

[15] Kim, K. K.,Hsu, A., Jia, X., Kim, S. M., Shi, Y., Hofmann, M., Nezich, D., Rodriguez-Nieva, J. F., Dresselhaus, M., Palacios, T., *et al*. Synthesis of monolayer hexagonal boron nitride on Cu foil using chemical vapor deposition. Nano Lett. 12, 161–166 (2012).

[16] Tay, R.Y., Griep, M.H., Mallick, G., Tsang, S.H., Singh, R.S., Tumlin, T. Tong Teo, E.H.T., Karna, S.P. Growth of large single-crystalline two-dimensional boron nitride hexagons on electropolished copper. Nano Lett 14, 839–846 (2014).

[17] Kim, G., Jang, A.R., Jeong, H.Y., Lee, Z., Kang, D.J., Shin, H.S. Growth of high-crystalline, single-layer hexagonal boron nitride on recyclable platinum foil. Nano Lett.=13, 1834–1839 (2013).

[18] Gao,Y., Ren, W., Ma, T., Liu, Z., Zhang, Y., Liu, W.B., Ma, L.P., Ma, X., Cheng, H.M. Repeated and controlled growth of monolayer, bilayer and few-layer hexagonal boron nitride on Pt foils. ACS Nano 7, 5199–5206 (2013).

[19] Mortazavi, B., Pötschke, M., Cuniberti, G. Multiscale modeling of thermal conductivity of polycrystalline graphene sheets. Nanoscale 6, 3344-3352 (2014).

[20] Huang, P.Y., Ruiz-Vargas, C.S., van der Zande, A.M., Whitney, W.S., Levendorf, M.P., Kevek, J.W., *et al.* Grains and grain boundaries in single-layer graphene atomic patchwork quilts. Nature 469, 389-392 (2011).

[21] Ruiz-Vargas, C.S., Zhuang, H.L., Huang, P.Y., van der Zande, A.M., Garg, S., McEuen, P.L., *et al.* Softened elastic response and unzipping in chemical vapor deposition graphene membranes. Nano Lett 11, 2259–2263 (2011).

[22] Lee, G.W., Cooper, R.C., An, S.J., Lee, S.,van der Zande, A.M., Petrone, N., Hammerberg, A.G., *et al.* High-strength chemical-vapor–deposited graphene and grain boundaries. Science 340, 1073-1076 (2013).

[23] Liu, Y., Yakobson, B.I. Cones, pringles, and grain boundary landscapes in graphene topology. Nano Lett 10, 2178−2183 (2010).

[24] Liu, Y., Zou, X.,Yakobson, B. I. Dislocations and grain Boundaries in two-dimensional boron nitride, ACS Nano 6, 7053-7058 (2012).

[25] Gibb, A.L., Alem, N., Chen, J.H., Erickson, K.J., Ciston, J., Gautam, A., Linck, M., Zettl, A., Atomic resolution imaging of grain boundary defects in monolayer chemical vapor deposition-grown hexagonal boron nitride. J. Am. Chem. Soc. 35, 6758–6761 (2013).

[26] Plimpton, S. Fast parallel algorithms for short-range molecular dynamics. J. Comp. Phys.117, 1-19 (1995).

[27] Tersoff, J. New empirical approach for the structure and energy of covalent systems. Phys. Rev. B 37, 6991-7000 (1998).

[28] Matsunaga, K., Fisher, C., Matsubara, H. Tersoff potential parameters for simulating cubic boron carbonitrides. Jpn. J. Appl. Phys. 39, 48-51(2000).

[29] Kotakoski, J., Meyer, J.C. Mechanical properties of polycrystalline graphene based on a realistic atomistic model. Phys. Rev. B 85, 195447 (2012).

[30] Brenner, D.W., Shenderova, O.A., Harrison, J.A., Stuart, S.J., Ni, B., Sinnott, S.B. A second-generation reactive empirical bond order (REBO) potential energy expression for hydrocarbons. J. Phys. Condens. Matter 14, 783–802 (2002).

[31] Warner, J.H., Rummeli, M.H., Bachmatiuk, A., Buchner, B. Atomic resolution imaging and topography of boron nitride sheets produced by chemical exfoliation. ACS nano 4,1299-1304 (2010).

[32] Humphrey, W., Dalke, A., Schulten, K., VMD - Visual Molecular Dynamics, J. Molec. Graphics 14, 33-38 (1996).

[33] Peng, Q., Ji, W., De, D.. Mechanical properties of the hexagonal boron nitride monolayer: Ab initio study. Comput. Mat. Sci. 56, 11-17 (2012).

[34] Wu, J., Wang, B., Wei, Y., Yang, R., Dresselhaus, M. Mechanics and Mechanically Tunable Band Gap in Single-Layer Hexagonal Boron-Nitride. Mater. Res. Lett. 1, 200–206 (2013).

[35] Kudin, K.N., Scuseria, G.E., Yakobson, B.I. C_2F, BN, and C nanoshell elasticity from ab initio computations. Phys. Rev. B 64, 235406 (2001).

[36] Hernandez, E., Goze, C., Bernier, P., Rubio, A. Elastic properties of C and $B_xC_yN_z$ composite nanotubes. Phys. Rev. Lett. 80, 4502 (1998).

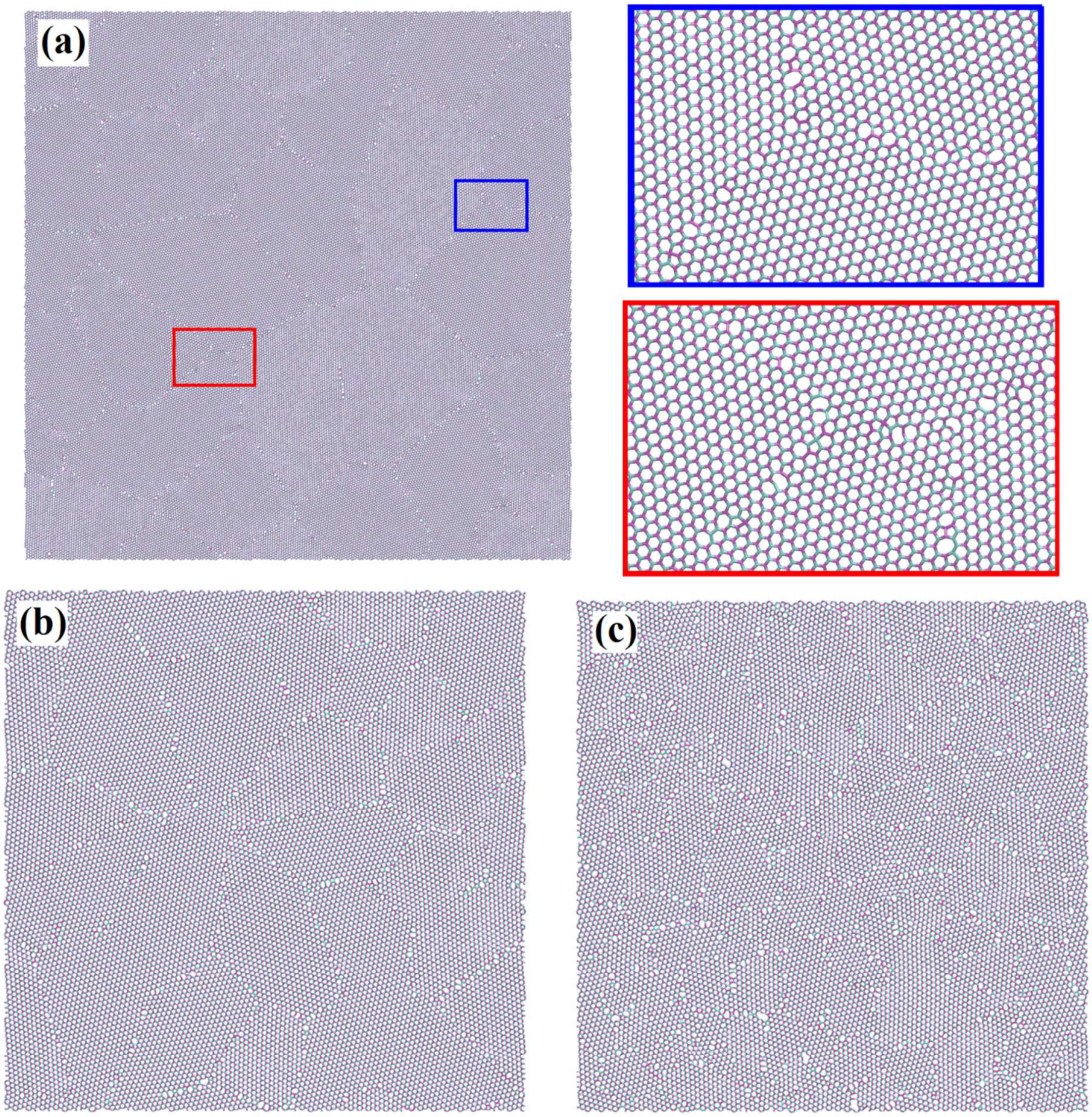

Fig. 1- Molecular models of periodic polycrystalline h-BN films with average grain size of (a) 10 nm (50 nm × 50 nm), (b) 5 nm (25 nm × 25 nm) and (c) 2nm (24 nm × 24 nm). VMD software [32] is used for graphical presentation of polycrystalline structures.

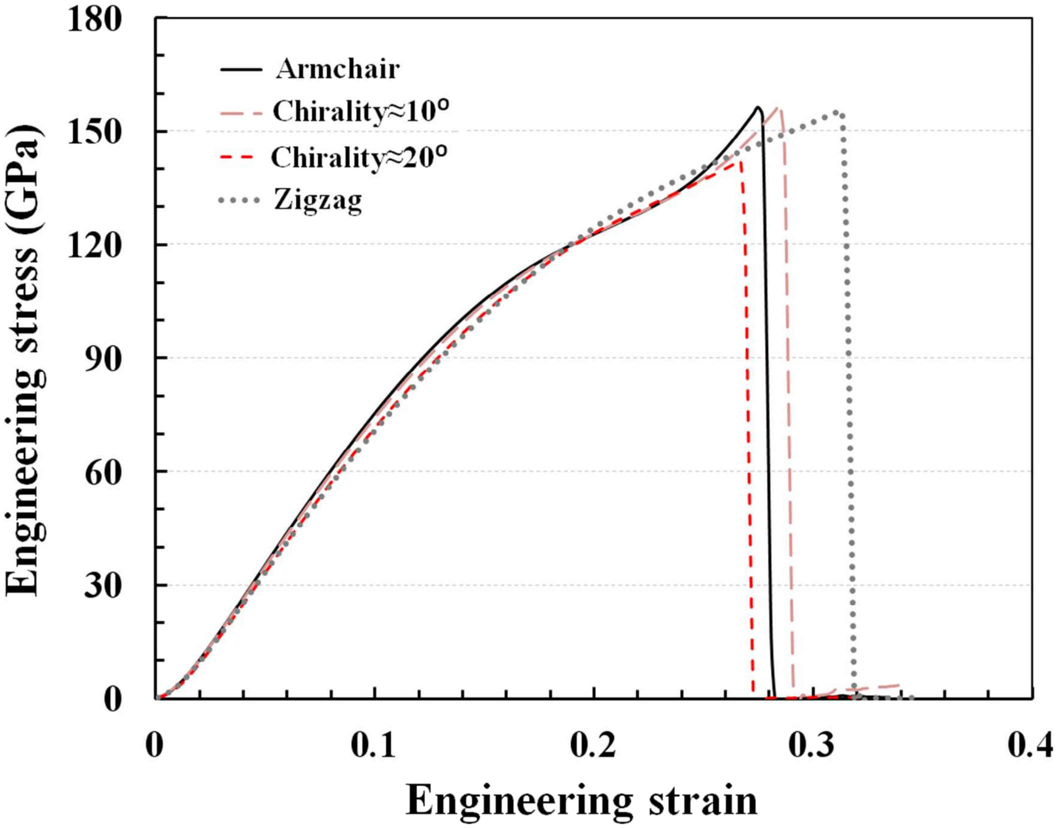

Fig. 2- Stress-strain response of defect-free single-layer h-BN along different loading directions.

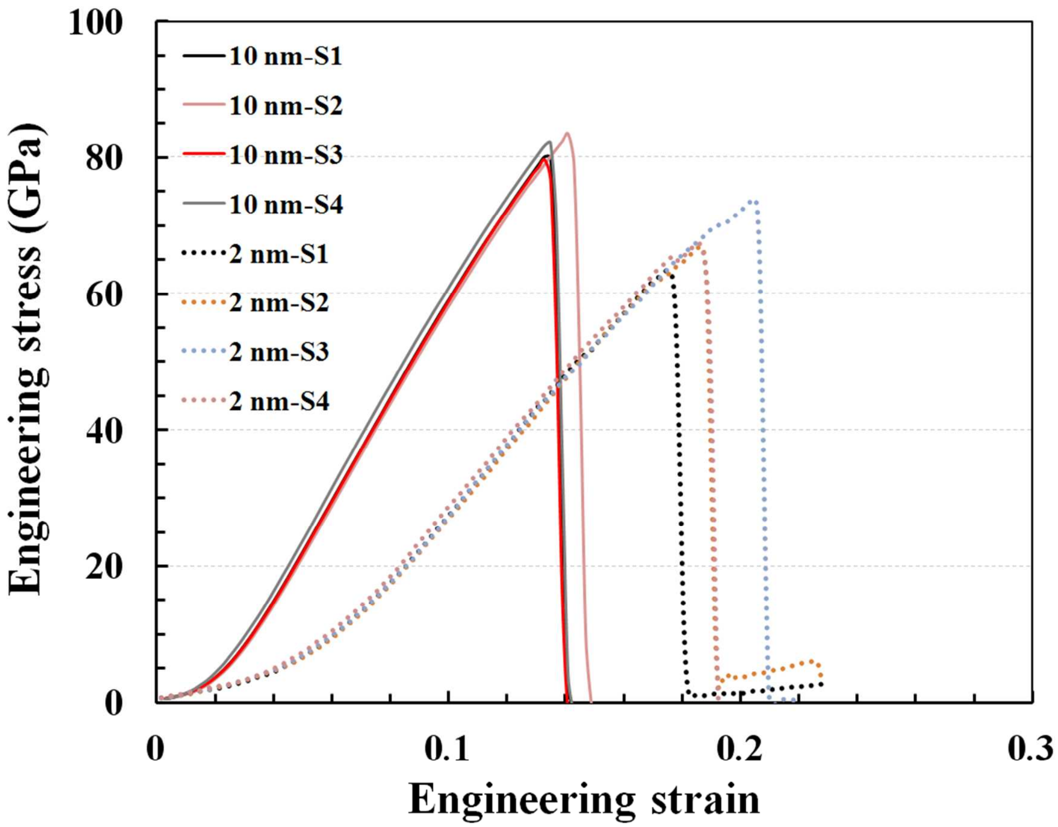

Fig. 3- Stress-strain response of polycrystalline h-BN sheets with average grain size of 2 nm and 10 nm for four different samples (S) with different grain configurations.

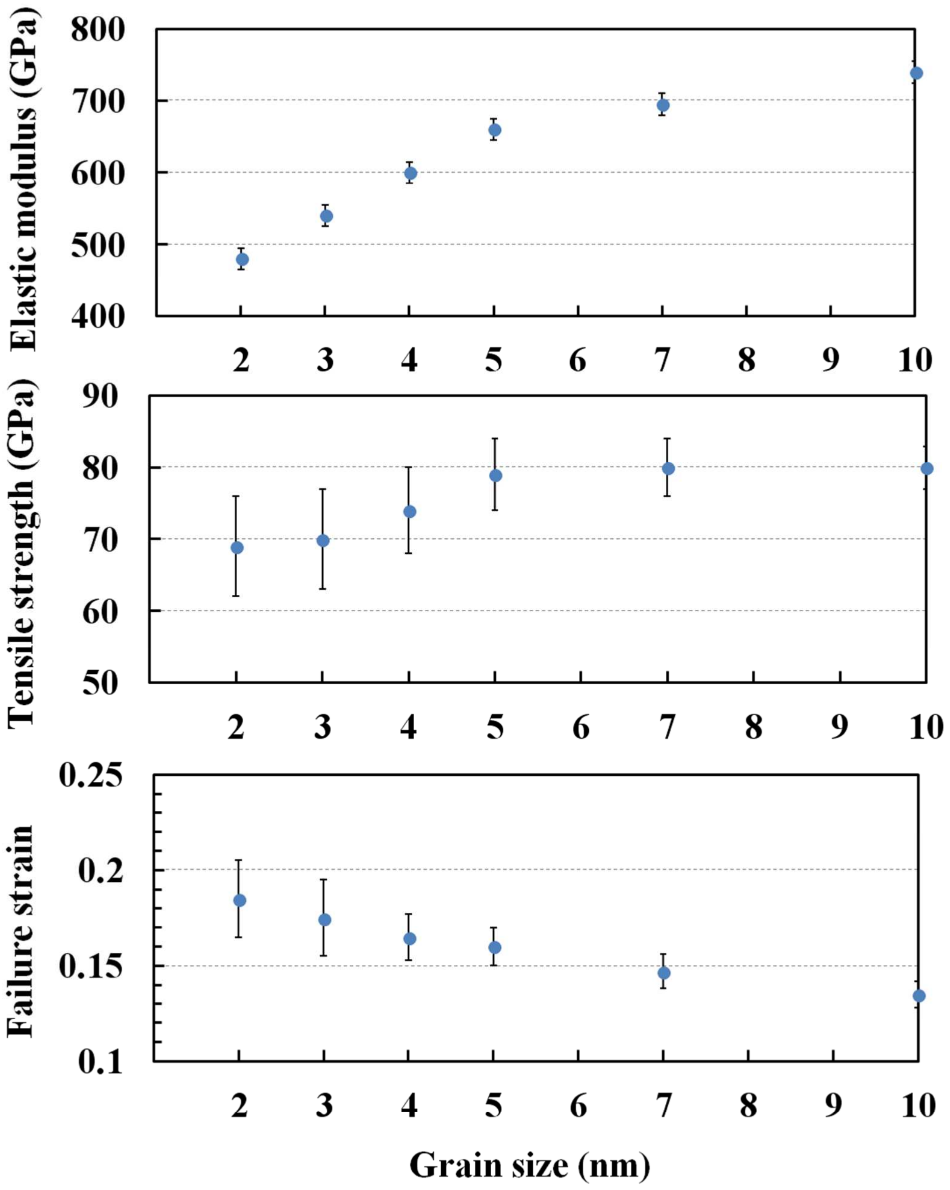

Fig. 4- Elastic modulus, tensile strength and failure strain of ultra-fine grained single-layer h-BN sheets as a function of grain size.

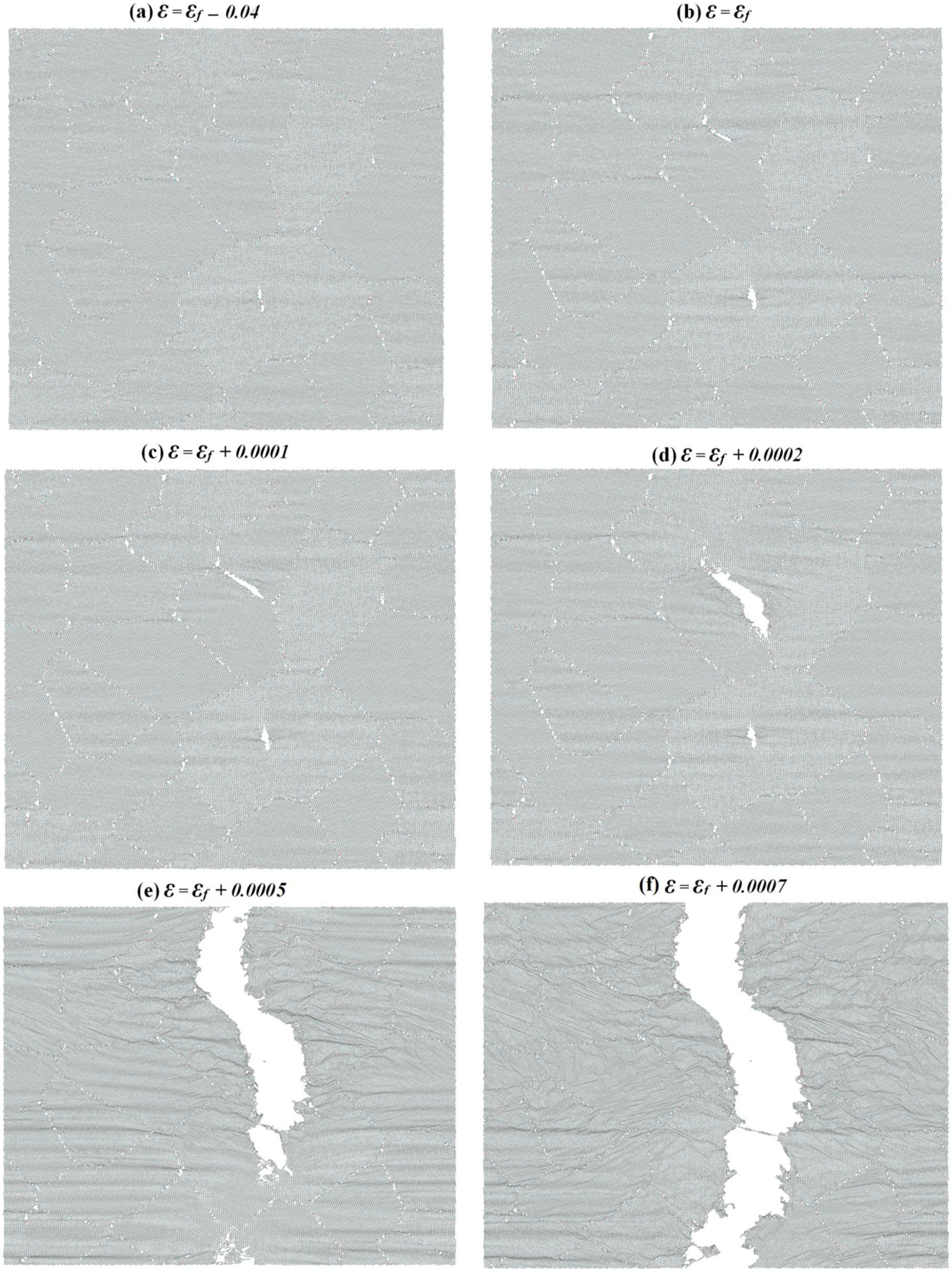

(a) $\varepsilon = \varepsilon_f - 0.04$

(b) $\varepsilon = \varepsilon_f$

(c) $\varepsilon = \varepsilon_f + 0.0001$

(d) $\varepsilon = \varepsilon_f + 0.0002$

(e) $\varepsilon = \varepsilon_f + 0.0005$

(f) $\varepsilon = \varepsilon_f + 0.0007$

Fig 5- Failure process of a polycrystalline h-BN sheet with an average grain size of 10 nm at different strain levels. Engineering strain value (ε) for each image is depicted by its relative engineering strain difference with respect to the sample's strain at ultimate strength (ε_f).